oscillators are all equal to $2\pi/n$. With the choice of parameters used in the experiment, Eq. (1) describes a reduced 3-node network system with $a_i = a$, $c_{ik} = c$, and $\gamma_{ik} = \gamma$ (values given in Fig. 1c), which has 3-fold rotational symmetry (as the original AC circuit). This system has two splay states (with identical $\lambda^{\max}$), corresponding to two fixed points of Eq. (1) for which the phase angles of the adjacent generators are exactly 120 degrees apart (i.e., $\delta_2 - \delta_1 = \pm 120°$ and $\delta_3 - \delta_1 = \mp 120°$). Each of these is a rotationally symmetric state of the system, since applying any rotational permutation of the generators would result in the same state (equivalent up to a uniform shift of all δ_i). In these states, the effective coupling pattern expressed in the matrix $\mathbf{P}$ takes a form that favors converse symmetry breaking (see Methods for details).

The stability landscape—the function $\lambda^{\max}(\boldsymbol{\beta}) = \lambda^{\max}(\beta_1, \beta_2, \beta_3)$—for the frequency-synchronous splay states of our experimental system exhibits the same rotational symmetry as the system itself, as illustrated in Fig. 1d assuming ideal system components (see Methods for details). Due to this symmetry, the landscape has global minima (all with the same $\lambda^{\max}$ value) at three different locations in the $\boldsymbol{\beta}$-space, related by a 120-degree rotation of the β_i-axes. One of these minima, which we denote by $\boldsymbol{\beta}_g$, is located approximately at $(3.69, 3.68, 5.18)$ and corresponds to a globally optimal (non-uniform) assignment of the generator parameters with $\lambda^{\max}(\boldsymbol{\beta}_g) \approx -1.67$. In contrast, the optimal uniform assignment (i.e., the optimum under the constraint $\beta_1 = \beta_2 = \beta_3$) corresponds to the point $\widetilde{\boldsymbol{\beta}} = (\widetilde{\beta}, \widetilde{\beta}, \widetilde{\beta})$ with $\widetilde{\beta} \approx 3.76$ and $\lambda^{\max}(\widetilde{\boldsymbol{\beta}}) \approx -1.46$. These two points are marked on the cross section of the stability landscape shown in Fig. 1e. Since condition (3) is satisfied for $\boldsymbol{\beta}^* = \boldsymbol{\beta}_g$, the system is predicted to exhibit converse symmetry breaking: the rotationally symmetric, frequency-synchronous splay states are necessarily unstable for any uniform β_i assignment (corresponding to a rotationally symmetric system), whereas they become stable for the non-uniform β_i assignment in $\boldsymbol{\beta}_g$ (corresponding to a non-rotationally symmetric system) for a range of noise intensities.

Specific uniform and non-uniform β_i assignments were implemented in our experiment by adjusting the frictional brakes on the generator shafts (see Supplementary Information, Sec. S1 on how friction relates to β_i). Due to the physical limitations and finite measurement accuracy, the precision of a β_i value that we could realize was ± 0.1 (see Supplementary Information, Sec. S2.1). In addition, changes in the parameters of generator–motor units over time due to external effects (e.g., heating) as well as inherent heterogeneity of the system components (despite being manufactured to be identical) can distort the landscape itself and thus shift the locations of $\boldsymbol{\beta}_g$ and $\widetilde{\boldsymbol{\beta}}$. Even though care was taken to minimize deviations from the designed values (see Methods), it would be experimentally challenging to realize these points exactly. Therefore,

we considered two points on the landscape that we were able to realize and confirm with measurements: $\boldsymbol{\beta}_A \equiv (3.4 \pm 0.1, 3.6 \pm 0.1, 3.5 \pm 0.1) \approx \widetilde{\boldsymbol{\beta}}$ and $\boldsymbol{\beta}_B \equiv (3.4 \pm 0.1, 3.6 \pm 0.1, 5.0 \pm 0.1) \approx \boldsymbol{\beta}_g$ (projections of both points are marked in Fig. 1e). Our theoretical predictions for the stability at these points are $\lambda^{\max}(\boldsymbol{\beta}_A) \approx -1.42$ and $\lambda^{\max}(\boldsymbol{\beta}_B) \approx -1.63$, which confirms the property $\lambda^{\max}(\boldsymbol{\beta}_B) < \lambda^{\max}(\boldsymbol{\beta}_A)$ that is predicted to enable converse symmetry breaking in the experiment.

To provide experimental evidence for converse symmetry breaking, we performed multiple experimental runs while measuring the terminal voltage of each generator with a voltage sensor circuit and concurrently processing the measurements (see Methods for details). These measurements yielded multiple time series of terminal voltage phasors (angles and magnitudes) and the corresponding electrical angles δ_i, both recorded at $3{,}320$ samples per second. The total recorded time span was ≈ 1.5 h each for the $\boldsymbol{\beta}_A$ and $\boldsymbol{\beta}_B$ configurations. For our analysis, we focused on segments of the time series in which the splay states were observed (allowing for a maximum of ± 10 degree deviation in δ_i; see Methods for the full details on this criterion). Since system parameters may fluctuate and shift gradually during an experimental run, we estimated a (slightly different) steady state for each segment using the averages of the measured phasor angles δ_i^* over all data points in the segment. Using these steady-state values, as well as measured system parameters, we estimated $\lambda^{\max}$ for each segment of each $\boldsymbol{\beta}$ configuration (see Methods for the procedure to calculate $\lambda^{\max}$).

The $\lambda^{\max}$ estimated from experimental data (shown in Fig. 3a) are distributed around the corresponding theoretical predictions for the splay states. The mean values of $\lambda^{\max}$ for the two configurations are significantly different, which we confirmed with the paired t-test; the null-hypothesis that the difference of the means is zero is rejected, because the p-value is smaller than machine precision and is certainly smaller than the significance level of 0.05. The difference between the two means (≈ 0.165) is substantially larger than a typical variation of $\lambda^{\max}$ along the trajectory in a segment (Supplementary Fig. 2a), indicating that our conclusion is not sensitive to uncertainty in the measurement of steady-state δ_i^* values.

In addition to establishing the statistically significant difference in the averaged $\lambda^{\max}$ between the two configurations, we investigated the extent to which changing the configuration from $\boldsymbol{\beta}_A$ to $\boldsymbol{\beta}_B$ enhances the stability of the same experimentally realized states. This was done by recomputing $\lambda^{\max}$ for $\boldsymbol{\beta} = \boldsymbol{\beta}_A$ and $\boldsymbol{\beta} = \boldsymbol{\beta}_B$ for each time-series segment, which is justified because the steady state of Eq. (1) does not depend on the choice of $\boldsymbol{\beta}$. Thus, the recomputed $\lambda^{\max}$ determines the stability we would observe if, starting with one $\boldsymbol{\beta}$ configuration, the brakes

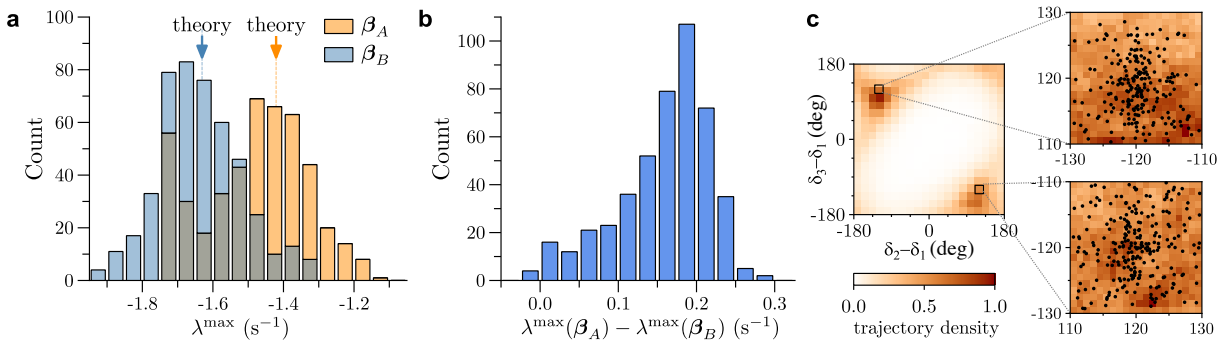

Fig. 3: **Experimental confirmation of converse symmetry breaking. a**, Distribution of the Lyapunov exponents $\lambda^{\max}$ obtained from individual time-series segments for the uniform ($\boldsymbol{\beta}_A$, orange histogram) and non-uniform ($\boldsymbol{\beta}_B$, blue histogram) configurations. For each segment, we used the measured splay state and associated parameters, and calculated $\lambda^{\max}$ as an average over that segment. The downward arrows indicate the predicted values of $\lambda^{\max}$ for the theoretically calculated splay states (in which the angles are exactly 120 degrees apart). **b**, Distribution of synchronization stability improvement achieved by changing the generator parameters from $\boldsymbol{\beta}_A$ to $\boldsymbol{\beta}_B$ for the same states, as measured by the difference $\lambda^{\max}(\boldsymbol{\beta}_A) - \lambda^{\max}(\boldsymbol{\beta}_B)$. **c**, Inferred splay states and density plot of time-series trajectories. The horizontal and vertical axes are the phase angles δ_2 and δ_3 of the second and third generators, respectively, relative to the first generator. The trajectory density was estimated for each pixel using all measured time series. The color scale is normalized to the highest measured density. The dots in the enlarged sections mark the steady splay states determined for the time-series segments we considered (275 and 190 segments for the $\boldsymbol{\beta}_A$ and $\boldsymbol{\beta}_B$ configurations, respectively).

on the generators were adjusted to realize the other configuration without changing the state. Finding $\lambda^{\max}(\boldsymbol{\beta}_B) < \lambda^{\max}(\boldsymbol{\beta}_A) < 0$ for a given steady state implies that condition (3) for converse symmetry breaking is satisfied for $\boldsymbol{\beta}^* = \boldsymbol{\beta}_B$ and $\widetilde{\boldsymbol{\beta}} \approx \boldsymbol{\beta}_A$. As shown in Fig. 3b, this was indeed observed to be the case for almost all the identified time-series segments (whose corresponding splay states inferred from data are shown in Fig. 3c). We also verified that the observed stability improvement is robust against uncertainties in generator parameters (Supplementary Fig. 2b). Thus, our measurements and analysis provide experimental evidence of converse symmetry breaking—a rotationally symmetric synchronous state of our system becomes stable when the rotational symmetry of the system is broken by the heterogeneity of the generator parameters.

Our demonstration of converse symmetry breaking can be interpreted from various different angles. On the one hand, it establishes a scenario in which stable symmetric states require system asymmetry. On the other hand, it shows that the assumption that increasing uniformity across individual entities would facilitate uniform behavior is generally false, even when they